Chinese J. Chem. Eng., **10** (2) 202 – 207 (2002)

Analyses of Multiplicity and Stability Patterns of Agglomeration Controlled Precipitation with Both Primary and Secondary Nucleations

YIN Qiuxiang(尹秋响), ZHANG Meijing(张美景) and WANG Jingkang(王静康)**
School of Chemical Engineering and Technology, Tianjin University, Tianjin 300072, China

Abstract The possibility of multiplicity in an isothermal continuous mixed suspension-mixed product removal crystallizer is explored using the bifurcation theory. A process involving agglomeration controlled precipitation is considered in which secondary nucleation occurs simultaneously with primary nucleation. The determinant equations for the existence of multiple steady states are developed and the multiplicity boundaries dependent on the physical and kinetic properties and operational parameters of the process are obtained by resolving these determinant equations. The number of steady states in the precipitator for various multiplicity regions is determined and the linear stability of these steady states is analyzed by using the Routh criterion.
Keywords precipitation, mixed suspension-mixed product removal crystallizer, agglomeration, multiplicity, stability

1 INTRODUCTION

The possible appearance of multiple steady states for continuous crystallization and reactive precipitation has been paid considerable attention in literature. Tavare *et al.*[1−3] applied the theories of multiplicity and stability to continuous mixed suspension-mixed product removal (CMSMPR) crystallizers and reactive precipitators, and derived implicit criteria for uniqueness and multiplicity of steady states of the systems. In allusion to these systems, Yin *et al.*[4−6] developed stricter explicit criteria for uniqueness and multiplicity based on rigorous moment equation models. Furthermore, Lakatos[7,8] studied the influence of nucleation mechanisms on the multiplicity behavior in an isothermal CMSMPR crystallizer. These investigations have dealt with systems in which only either primary or secondary nucleation occurs, but less attention was paid to the case of simultaneous occurrence of primary and secondary nucleation. In light of these situations, Yin *et al.*[9,10] investigated the multiplicity and transient behavior of an isothermal CMSMPR crystallizer with both primary and secondary nucleations. On the other hand, in all of these works, it is assumed that the particle size is controlled by molecular growth. However, it has been recognized that for many precipitation processes particle agglomeration plays an important even a dominant role in establishing the product size distribution[11]. Therefore, in Padia and Bhatia's work[12], the possibility of multiplicity for agglomeration controlled precipitation with primary or secondary nucleation was studied separately. They found that primary nucleation might lead to three steady states while secondary nucleation lead to as many as four steady states.

The present study is aimed at investigating the multiplicity behavior of agglomeration controlled precipitation process with both primary and secondary nucleations in an isothermal CMSPMR crystallizer. The specific objective of this work is to determine the parameter regions over which multiple steady states occur and to analyze the stability of these steady states.

2 MODEL DEVELOPMENT

2.1 Population and solute balances

In the present analysis, an isothermal CMSMPR precipitator with clear and solid-free feed stream is considered. We assume agglomeration dominant precipitation with negligible molecular growth and breakage. Furthermore, it is assumed that precipitated particles are nucleated in a finite volume v_b. Under these conditions it is quite convenient to use the particle volume as the internal coordinate to phrase the population balance as following[11]

$$\frac{\partial n(v,t)}{\partial t} = -\frac{n(v,t)}{\tau} + B_a - D_a + B\delta(v - v_b) \quad (1)$$

in which the agglomeration-related terms B_a and D_a can be formulated analogously to the formulation of coalescence of aerosols[11].

The solute balance based on the mass of solvent leads to

$$\frac{d(c + M_T)}{dt} = \frac{1}{\tau}(c_f - c - M_T) \quad (2)$$

in which the magma density, M_T, is related to n, v and ρ by

$$M_T = k_v \rho \int_0^\infty v n(v,t) dv \quad (3)$$

Received 2001-02-27, accepted 2001-07-16.
* To whom correspondence should be addressed.

2.2 Nucleation kinetics

The nucleation of crystals is a complex process by itself, behind which different mechanisms may be expressed by significantly differing rate equations[11]. If a crystallizer is operated with high supersaturation and low magma density, new particles are born dominantly by primary nucleation. While in the case of low supersaturation and high magma density, secondary nucleation appears to be the dominating process producing new crystals. These two kinds of nucleation mechanisms provide two extremes of the process behavior. Knowledge of the process behavior may also be of importance in situations where both nucleation phenomena proceed at comparable rates. In the precipitator under consideration, primary and secondary nucleation processes take place simultaneously, and the overall nucleation rate is described by

$$B = k_{\mathrm{p}}\exp\left[-\frac{K}{(c/c_{\mathrm{e}}-1)^2}\right] + k_{\mathrm{b}}(c-c_{\mathrm{e}})^b M_{\mathrm{T}}^j \quad (4)$$

where the first term is the Volmer model for primary homogeneous nucleation and the second one is the magma dependent power law model for secondary nucleation. According to Garside[13], the Volmer model is also satisfactory for primary heterogeneous nucleation but with a lower value of K due to the reduction in surface energy at heterogeneous nucleation sites.

From energy considerations[14], the nucleus volume v_{b} is obtained as

$$v_{\mathrm{b}} = \frac{2K}{\rho N_{\mathrm{av}}[\ln(c/c_{\mathrm{e}})]^3} \approx \frac{2K}{\rho N_{\mathrm{av}}(c/c_{\mathrm{e}}-1)^3} \quad (5)$$

at which size the gain in free energy due to formation of solid becomes large enough to overcome the loss in free energy associated with the creation of a new interface.

2.3 Model equations

Because of the appearance of the first moment of $n(v,t)$ in Eqs. (2) and (3) , it is more convenient to transform Eqs. (1) and (2) in the moment form by defining

$$m_1 = \int_0^\infty v n(v,t)\mathrm{d}v \quad (6)$$

Thus, we obtain (see Appendix for details)

$$\frac{\mathrm{d}m_1}{\mathrm{d}t} = -\frac{m_1}{\tau} + Bv_{\mathrm{b}} \quad (7)$$

$$\frac{\mathrm{d}c}{\mathrm{d}t} = \frac{1}{\tau}(c_{\mathrm{f}}-c) - k_{\mathrm{v}}\rho B v_{\mathrm{b}} \quad (8)$$

An interesting outcome of the transformation is that since agglomeration conserves particle volume, and Eq. (7) is merely a solid phase volume balance, the agglomeration terms are no longer in the picture. Thus the dynamics of the first moment is independent of the agglomeration-related terms B_{a} and D_{a}.

For ease of analysis we introduce the following set of dimensionless variables and parameters

$$\begin{aligned}
\alpha &= 2k_{\mathrm{v}}k_{\mathrm{b}}\tau(c_{\mathrm{f}}-c_{\mathrm{e}})^{b+j-2}c_{\mathrm{e}}N_{\mathrm{av}}^{-1}\\
\beta &= k_{\mathrm{p}}/[k_{\mathrm{b}}(c_{\mathrm{f}}-c_{\mathrm{e}})^{b+j}]\\
F &= Kc_{\mathrm{e}}^2/(c_{\mathrm{f}}-c_{\mathrm{e}})^2\\
x &= k_{\mathrm{v}}\rho(c_{\mathrm{f}}-c_{\mathrm{e}})^{-1}m_1\\
y &= (c-c_{\mathrm{e}})/(c_{\mathrm{f}}-c_{\mathrm{e}})\\
\theta &= t/\tau
\end{aligned}$$

Notice that the dimensionless parameters α and β represent the relative importance of primary and secondary nucleation in the precipitation process. We estimate that the value of α can range widely from 0 to 10 and β from 0 to infinity. If $\alpha = 0$, $\beta \to \infty$, primary nucleation would be the dominating process for producing new crystals, while in the case of $\beta = 0$ new particles are born dominantly by secondary nucleation. Otherwise, both nucleation processes would simultaneously occur at comparable rates. F can be interpreted as a measure of the nonlinearity of the primary nucleation rate and is also a prime determinant in the gross level of primary nucleation. According to Jerauld *et al.*[15], F can range from 0.002 to 10 industrially and experimentally.

Recasting Eqs. (7) and (8) in dimensionless form and combining with Eqs. (4) and (5) yield

$$\frac{\mathrm{d}x}{\mathrm{d}\theta} = -x + \alpha\left[\beta\exp\left(-F/y^2\right) + y^b x^j\right]\left(F/y^3\right) \quad (9)$$

$$\frac{\mathrm{d}y}{\mathrm{d}\theta} = 1 - y - \alpha\left[\beta\exp\left(-F/y^2\right) + y^b x^j\right]\left(F/y^3\right) \quad (10)$$

The combined effect of physical properties and operation parameters on the dynamics of the state variables can be determined by simultaneously solving the model Eqs. (9) and (10) with appropriate initial conditions. At steady state, these equations yield

$$\begin{aligned}
&f_1(x_{\mathrm{s}}, y_{\mathrm{s}}, \boldsymbol{P}) =\\
&-x_{\mathrm{s}} + \alpha\left[\beta\exp\left(-F/y_{\mathrm{s}}^2\right) + y_{\mathrm{s}}^b x_{\mathrm{s}}^j\right](F/y_{\mathrm{s}}^3) = 0
\end{aligned} \quad (11)$$

$$f_2(x_{\mathrm{s}}, y_{\mathrm{s}}, \boldsymbol{P}) = 1 - y_{\mathrm{s}} - x_{\mathrm{s}} = 0 \quad (12)$$

which, along with the given physical properties, nucleation kinetic and operational parameters, can be solved simultaneously to yield steady state solutions. Here $\boldsymbol{P}$ is the parameter vector comprised of α, β, F, b and j.

3 MULTIPLICITY AND STABILITY ANALYSIS

3.1 Steady state multiplicity

The nonlinearity of the nucleation kinetics and the model equations discussed above, as well as the interactions between the kinetics and the particle size distribution, may give rise to possibility of multiple

steady states in the continuous precipitation system. To obtain the multiplicity boundaries, conventional bifurcation analysis[16,17] can be used to classify the parameter space into regions with different number of steady state solutions. The "bifurcation set" of parameter $\boldsymbol{P}$ can be determined by setting

$$\det \boldsymbol{J}(x_s, y_s, \boldsymbol{P}) = 0 \tag{13}$$

where $\boldsymbol{J}$ is the Jacobian matrix of Eqs. (11) and (12), namely

$$\boldsymbol{J} = \begin{bmatrix} \partial f_1/\partial x_s & \partial f_1/\partial y_s \\ \partial f_2/\partial x_s & \partial f_2/\partial y_s \end{bmatrix} \tag{14}$$

On simplification, Eq. (13) reduces to

$$4 + 2Fx_s y_s^{-3} - 3/y_s + \alpha F y_s^{b-6} x_s^{j-1}(b y_s^2 x_s - j y_s^3 - 2Fx_s) = 0 \tag{15}$$

Thus, the multiplicity boundaries, which would demarcate the parameter space into regions with different number of steady states, can be obtained by simultaneously solving the determinant Eqs. (11), (12) and (15).

3.2 Linearized stability analysis

To assess the stability of the steady state solutions, the model equations [Eqs. (9) and (10)] are linearized around the steady state and the sign of the eigenvalues of the Jacobian matrix is examined. The characteristic polynomial of the Jacobian determinant is

$$\boldsymbol{P}(\lambda) = \det(\boldsymbol{J} - \lambda \boldsymbol{I}) = \lambda^2 + a_1\lambda + a_2 \tag{16}$$

where

$$a_1 = 2 - \alpha F j y_s^{b-3} x_s^{j-1} \tag{17}$$

$$a_2 = 4 + 2Fx_s y_s^{-3} - 3y_s + \alpha F y_s^{b-6} x_s^{j-1}(\alpha b y_s^2 x_s - j y_s^3 - 2Fx_s) \tag{18}$$

According to the stability theory [17], to keep the system stable, real parts of the eigenvalues of the characteristic Eq. (16) must be negative. Applying the classical Routh criteria[17], it is found that for stability all the coefficients of the characteristic equation must be of the same sign, *i.e.*, a_1 and a_2 should be positive. For the present case this is the necessary as well as the sufficient condition for stability.

4 RESULTS AND DISCUSSION

4.1 Steady state multiplicity

The various dimensionless parameters of the process model based on simultaneous occurrence of primary and secondary nucleations and agglomeration controlled growth mechanism are α, β, F, b and j. Among these, α, β and F are operational parameters which can be varied by changing the inlet concentration and residence time, respectively. Of course, they are also functions of the kinetic parameters of the precipitation process. Parameters b and j correspond respectively to the extent of the dependence of the second nucleation rate on supersaturation and magma. The typical range of b and j can be taken as 1—4 and 0—2 respectively based on the data found in the literature[11].

Types of possible multiplicity behavior and the regions with multiple steady states are determined based on the values of these parameters. As discussed in the previous section, the multiplicity boundaries can be obtained by simultaneously solving the multiplicity criterion [Eq. (15)] and the steady state equations [Eqs. (11) and (12)]. For various values of β and F, Figs. 1(a) and (b) illustrate the multiplicity boundaries and the "boundary set"[16] as plots of α *versus* b for the cases of $j < 1$ and $j > 1$, respectively. It is shown that the multiplicity boundaries (solid line in Fig. 1) along with the "boundary set" (dashed line in Fig. 1) separate the parameter space into different regions of multiplicity. We categorized them into four types based on the range of the parameters considered and the nature of the multiplicity boundary. It is important to note that the "boundary set" which exists at $b = 3$ in the parameter space plots is independent of α, β, F and j and that the nature of the multiplicity boundaries is mainly dependent on the values of j and b. For magma power exponent less than unity, a multiplicity boundary exists only for $b < 3$ and this multiplicity boundary along with the "boundary set" at $b = 3$ divides the parameter space into three types of multiplicity regions [Fig. 1(a)]. However, the instance for the case of $j > 1$ is far more complicated. From Fig. 1(b), besides the multiplicity boundary existing for $b < 3$ and the "boundary set" at $b = 3$ similar to the previous case, there exist other two multiplicity boundaries for $b > 3$ and these two multiplicity boundaries intersect at a critical point with $b = b_{cr}$. Thus, for magma order greater than one the parameter space is classified into four regions. That is to say, if $b < 3$, the instance of regions demarcation for the case of $j < 1$ is similar to that for the case of $j > 1$, while if $b > 3$, the multiplicity boundary exists only for the case of $j > 1$, as can be seen from Figs. 1(a) and (b).

4.2 Bifurcation behavior

To show the bifurcation behavior of the system, nonlinear algebraic equations (11) and (12) are solved by using the continuation technique improved by Kubicek and Marek[17]. Following Kubicek and Marek's procedure, we can obtain the whole relationship between the steady state solutions of the model equations and the variable parameters in the parameter space of interest. As examples, the schematic bifurcation diagrams for dimensionless magma density x_s *versus* the operational parameter α for four typical sets of dimensionless parameters are shown in Fig. 2.

The stability of the steady states was examined by the above stability condition, and it is indicated by solid lines for stable and dashed lines for unstable in Fig. 2.

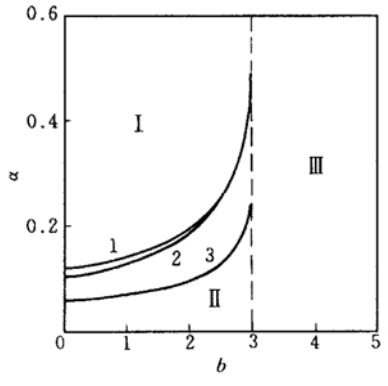

(a) $j = 0.5$

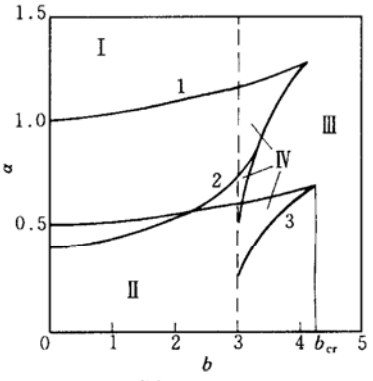

(b) $j = 1.5$

Figure 1 Multiplicity boundary as the plot of α *versus* b for different kinetic and operational parameters

1—$\beta = 0.1$, $F = 2$; 2—$\beta = 1$, $F = 2$; 3—$\beta = 1$, $F = 4$

- - - - boundary set; —— multiplicity boundary

From Figs. 2(a) and (b), it is seen that for the case of $b < 3$ the system exhibits the similar bifurcation behavior in spite of the value of j used. The bifurcation diagram is consisted of a stable and an unstable branches and these two branches meet at a limit point. This means when α is less than its value at the limit point, α^*, there are a stable and an unstable steady states; otherwise there is none.

When $b > 3$, however, the bifurcation behavior is comparatively complicated. If $j < 1$, the system has only one stable steady state over the whole range of α and with increase in operating parameter α the product rate increases steadily and continuously [Fig. 2(c)]. If $j > 1$ and $b > b_{cr}$ [the critical value of b in region IV of Fig. 1(b)], the system would exhibit only one stable steady state over the whole range of α and the bifurcation diagram is similar to Fig. 2(c). Otherwise, if $j > 1$ and $3 < b < b_{cr}$, the bifurcation diagram is consisted of three branches and the middle unstable one intersects with other two stable ones at two different limit points, as shown in Fig. 2(d). This means if α lies

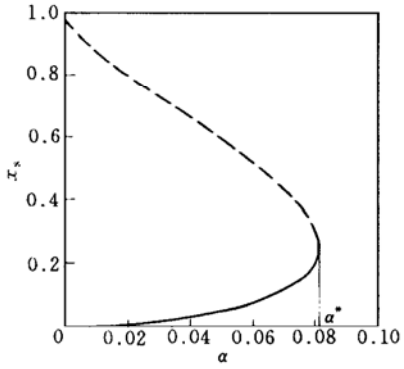

(a) $j = 0.5$, $b = 1.5$, $F = 4$, $\beta = 1$

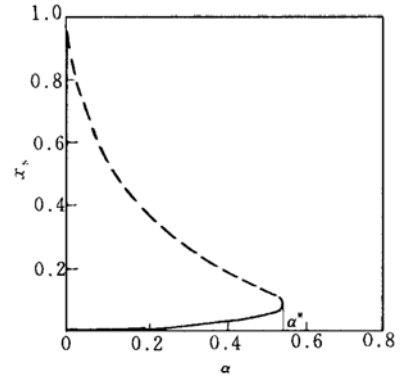

(b) $j = 1.5$, $b = 1.5$, $F = 4$, $\beta = 1$

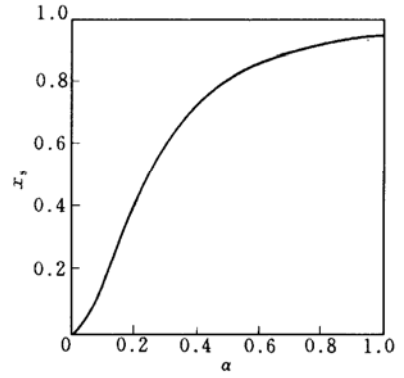

(c) $j = 0.5$, $b = 3.5$, $F = 4$, $\beta = 1$

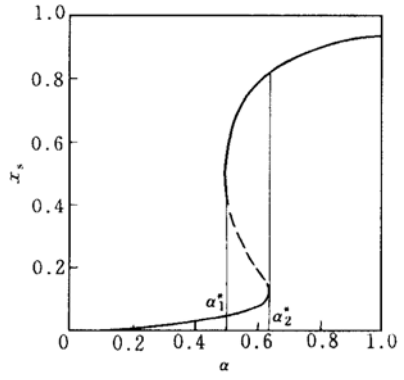

(d) $j = 1.5$, $b = 3.5$, $F = 4$, $\beta = 1$

Figure 2 Bifurcation diagram of dimensionless magma density x_s *versus* operational parameter α

- - - - unstable; —— stable

between these two limit points, namely $\alpha_1^* < \alpha < \alpha_2^*$, there exist two stable and an unstable steady states; otherwise there is only a stable one.

4.3 Discussion

According to the demarcation of multiplicity regions and bifurcation behaviors of the system in the different parameter regions, the number of steady states as well as their nature in the different regions of multiplicity indicated in Fig. 1 is outlined in Table 1. It is obvious that this result is completely consistent with the bifurcation theory[17]. Namely, when the parameter vector passes through the "boundary set" from one multiplicity region to another, the number of steady states would increase or decrease by "1", whereas when it passes through the multiplicity boundary, an increase or decrease by "2" would be expected.

Table 1 Number of stable and unstable steady states for various multiplicity regions as indicated in Fig. 1

Region	I	II	III	IV
stable	0	1	1	2
unstable	0	1	0	1

Region II in Fig. 1 enclosed by the multiplicity boundary, the "boundary set" at $b = 3$ and the coordinate axes exhibits two steady states, of which only the one corresponding to the lower production is stable [see Figs. 2(a) and (b)]. With increase in operating parameter α for the case of $b < 3$ transition from region II to region I occurs, then the system does not have any steady state. Region III in Fig. 1 is a more realistic area for precipitation studies. Here only one unique stable steady state is possible. However region IV of Fig. 1(b) for $j > 1$, trapped between the multiplicity boundaries and the "boundary set" at $b = 3$, exhibits three steady states of which the middle one is always unstable [Fig. 2(d)]. In this region, the bifurcation plots obtained for steady state variation with respect to operating parameter α reveal a hysteresis nature and the production rate between the two stable steady states varies with a several-fold difference. As can be seen from Fig. 2(d), for a start-up condition corresponding to a low value of operating parameter α, the system is likely to attain a low production steady state. For the start-up condition with high value of α, the system will attain a high production steady state. However, for medial value of operating parameter α, namely $\alpha_1^* < \alpha < \alpha_2^*$, the system can dramatically shift from low production to high production and *vice versa* depending on the magnitude of disturbance and the start up condition.

From Fig. 1(b) with decrease in β or increase in F, region IV expands, leading to multiplicity over a larger range of α. According to Eq. (4), decrease in β or increase in F means that secondary nucleation becomes more important than primary nucleation. That is to say, the lager the relative rate of secondary nucleation, the more possibility for multiplicity situations in agglomeration controlled precipitation. Similar conclusion was previously obtained by Yin *et al.*[9] for molecular growth controlled crystallization in which secondary nucleation occurs simultaneously with primary nucleation.

Here it is necessary to remark the relationship of this present study with Padia and Bhatia's work[12]. Padia and Bhatia[12] provided two extreme situations of our present study. If our analysis is extended to these extreme situations, the similar conclusions would be reached. It is noticeable that our analysis is based on the mass of solvent while Padia and Bhatia developed their model based on the volume of slurry.

Finally, it is important to assess the practical implications of the present work. The analysis indicates that an isothermal CMSMPR crystallizer involving agglomeration controlled precipitation with both primary and secondary nucleations may exhibit a wide variety of steady-state behavior. Although the parameter ranges within which the multiplicity might occur are narrow and the phenomenon of the multiplicity is limited to some special cases or to localized situations, a prior knowledge of the multiplicity regions is useful in the design, start-up and control of a precipitation process. Designers should be aware of these regions in order to avoid some false choices of operation parameters whereby the precipitator might be operated at conditions quite different from those intended.

5 CONCLUSIONS

A model for the investigation of multiplicity and stability patterns of agglomeration controlled precipitation with both primary and secondary nucleations in an isothermal CMSMPR crystallizer is developed. The analysis solely based on steady state balances indicates that there may be multiple steady states. Among the kinetic and operating parameters, α, b and j appear to be the crucial parameters with significant influence on the multiplicity and bifurcation behaviors. The parameter space can be classified into four multiplicity regions in which the number of steady states ranges from 0 to 3. The results of linear stability analysis show that in the case of two steady states system, the state with high production would be unstable, and for the three steady states system, the middle one would be unstable.

NOMENCLATURE

a_1, a_2	coefficients in the characteristic Eq. (16)
B	overall nucleation rate based on the mass of solvent, no.·s^{-1}·g^{-1}
B_a	birth rate of particles due to agglomeration, no.·s^{-1}·g^{-1}
b	kinetic order in nucleation rate
b_{cr}	critical value of b in region IV of Fig. 1(b)

c	concentration based on the mass of solvent, $g \cdot g^{-1}$
D_a	death rate of particles due to agglomeration, $no. \cdot s^{-1} \cdot g^{-1}$
F	dimensionless parameter $[F = Kc_e^2/(c_f - c_e)^2]$
f_1, f_2	dimensionless function
$\boldsymbol{I}$	identity matrix
$\boldsymbol{J}$	Jacobian matrix
j	magma order in nucleation rate
K	constant in Volmer's nucleation law
k_b	secondary nucleation rate constant, $no. \cdot s^{-1} \cdot g^{-1}$
k_p	primary nucleation rate constant, $no. \cdot s^{-1} \cdot g^{-1}$
k_v	volume shape factor
M_T	magma density based on the mass of solvent, $g \cdot g^{-1}$
m_1	firth moment of $n(v,t)$
N_{av}	Avogadro's number
$n(v,t)$	particle density distribution function based on the mass of solvent, $no. \cdot g^{-1}$
$\boldsymbol{P}$	parameter vector
t	time, s
v	particle volume, m^3
v_b	nucleus volume, m^3
x	dimensionless magma density
y	dimensionless concentration
α	operational parameter
α^*	α value at the limit point
β	dimensionless parameter $\{[\beta = k_p/[k_b(c_f - c_e)^{b+j}]\}$
δ	Dirac delta function
θ	dimensionless time
λ	eigenvalue of the characteristic matrix
ρ	particle density, $g \cdot m^{-3}$
τ	mean residence time, s

Subscripts

f	feed
e	saturation
s	steady state value

REFERENCES

1 Tavare, N. S., Garside, J., "Multiplicity in continuous MSMPR crystallizers. Part I. Concentration multiplicity in an isothermal crystallizer", *AIChE J.*, **31**, 1121 (1985).

2 Tavare, N. S., Garside, J., Akoglu, K., "Multiplicity in continuous MSMPR crystallizers. Part II. Temperature multiplicity in a cooling crystallizer", *AIChE J.*, **31**, 1128 (1985).

3 Tavare, N. S., "Multiplicity in continuous crystallizers: Adiabatic reactive precipitation", *Chem. Eng. Comm.*, **80**, 135 (1989).

4 Yin, Q. X., Wang, J. K., Wang, Y. L., "Multiplicity in continuous MSMPR crystallizers", *J. Chem. Ind. Eng. (China)*, **48**, 692 (1997). (in Chinese)

5 Yin, Q. X., "Multiplicity in continuous adiabatic MSMPR reactive precipitators", *Chinese J. Chem. Eng.*, **6**, 138 (1998).

6 Yin, Q. X., Wang, J. K., Xu, Z., Li, G. Z., "Analysis of concentration multiplicity patterns of continuous isothermal mixed suspension-mixed product removal reactive precipitators", *Ind. Eng. Chem. Res.*, **39**, 1437 (2000).

7 Lakatos, B. G., "Influence of nucleation mechanisms on the multiplicity of steady states in isothermal CMSMPR crystallizers", *React. Kinet. Catal. Lett.*, **47**, 305 (1992).

8 Lakatos, B. G., "Uniqueness and multiplicity in isothermal MSMPR crystallizers", *AIChE J.*, **42**, 285 (1996).

9 Yin, Q. X., Wang, J. K., Zhang, M. J., "Analyses of multiplicity and transient patterns of isothermal CMSMPR crystallizers (I). Conditions for the existence of multiplicits and the appearance of sustained oscillations", *J. Chem. Ind. Eng. (China)*, **53** (4), 390—394 (2002). (in Chinese)

10 Yin, Q. X., Zhang, M. J., Wang, J. K., Xu, Z., "Analyses of multiplicity and transient patterns of isothermal CMSMPR crystallizers (II). Bifurcation behavior and transient characteristics", *J. Chem. Ind. Eng. (China)*, **53** (4), 395—4000 (2002). (in Chinese)

11 Randolph, A. D., Larson, M. A., Theory of Particulate Processes, 2nd edition., Academic Press, New York (1988).

12 Padia, B. K., Bhatia S. K., "Multiplicity and stability analysis of agglomeration controlled precipitation", *Chem. Eng. Comm.*, **104**, 227 (1991).

13 Garside, J., "Industrial crystallization from solution", *Chem. Eng. Sci.*, **40**, 3 (1985).

14 Nielsen, A. E., "Nucleation and growth of crystals at high supersaturation", *Kristall. Technik.*, **4**, 17 (1969).

15 Jerauld, G. R., Vasatis, Y., Doherty, M. F., "Simple conditions for appearance of sustained oscillations in continuous crystallizers", *Chem. Eng. Sci.*, **38**, 1675 (1983).

16 Balakotaiah, V., "Steady state multiplicity features of open chemically reacting systems", *Lect. Appl. Math.*, **24**, 129 (1986).

17 Kubicek, M., Marek, M., Computational Methods in Bifurcation Theory and Dissipative Structures, Spring-Verlag, New York (1983).

APPENDIX

Derivation of Eqs. (7) and (8)

Multiply Eq. (1) by v and integrate each term with respect to v between the limits leads to

$$\int_0^\infty v\frac{\partial n(v,t)}{\partial t}\mathrm{d}v = -\int_0^\infty v\frac{n(v,t)}{\tau}\mathrm{d}v + \int_0^\infty (B_a - D_a)v\mathrm{d}v + B\int_0^\infty v\delta(v - v_b)\mathrm{d}v \tag{A1}$$

In Eq. (A1)

$$\int_0^\infty v\frac{\partial n(v,t)}{\partial t}\mathrm{d}v = \frac{\mathrm{d}m_1}{\mathrm{d}t} \tag{A2}$$

$$\int_0^\infty v\frac{n(v,t)}{\tau}\mathrm{d}v = \frac{m_1}{\tau} \tag{A3}$$

$$\int_0^\infty (B_a - D_a)v\mathrm{d}v = 0 \tag{A4}$$

since agglomeration conserves particle volume.

$$\int_0^\infty v\delta(v - v_b)\mathrm{d}v = \int_0^\infty (v - v_b)\delta(v - v_b)\mathrm{d}v + v_b\int_0^\infty \delta(v - v_b)\mathrm{d}v = 0 + v_b \tag{A5}$$

Therefore, Eq. (A1) leads to Eq. (7).

Recasting Eq. (2) in terms of the moment of $n(v,t)$ leads to

$$\frac{\mathrm{d}c}{\mathrm{d}t} = \frac{1}{\tau}(c_f - c) - k_v\rho\left(\frac{\mathrm{d}m_1}{\mathrm{d}t} + \frac{m_1}{\tau}\right) \tag{A6}$$

Substituting Eq. (7) in Eq. (A6) leads to Eq. (8).